Lithos 127 (2011) 441–454

Contents lists available at SciVerse ScienceDirect

Lithos

journal homepage: www.elsevier.com/locate/lithos

Bulk rock and mineral chemistries and ascent rates of high-K calc-alkalic epidote-bearing magmas, Northeastern Brazil

R.G. Brasilino [a,1], A.N. Sial [a,*], V.P. Ferreira [a], M.M. Pimentel [b]

[a] NEG-LABISE, Department of Geology, Federal University of Pernambuco, C.P. 7852, CEP 50670-000, Recife, PE, Brazil
[b] Institute of Geosciences, Federal University of Rio Grande do Sul, Porto Alegre, RS, 91509-900, Brazil

ARTICLE INFO

Article history:
Received 21 January 2011
Accepted 23 September 2011
Available online xxxx

Keywords:
Magmatic epidote
Rapid magma ascent
Neoproterozoic
Bulk chemistry
Mineral chemistry

ABSTRACT

A manifestation of the Pan-African-Brasiliano orogeny (700–550 Ma) in northeastern Brazil was the emplacement of widespread Neoproterozoic granitoids in diverse tectonic terranes. Among these plutons are the magmatic epidote-bearing Conceição das Creoulas, Caldeirão Encantado, Murici, and Boqueirão plutons, located close to the boundary between the Alto Pajeú and Cachoeirinha–Salgueiro terranes. The plutons are high-K calc-alkalic granodiorites to monzogranites, with tabular K-feldspar megacrysts.

Pistacite [atomic $Fe^{+3}/(Fe^{3+}+Al)$] in epidote in these granitoids ranges from 21 to 27%. High oxygen fugacity (log fO_2 −19 to −13) and the preservation of epidote suggest that the magma was oxidized. Al-in-hornblende barometry indicates hornblende solidification between 6 and 8 kbar, at 620 to 780 °C according to the hornblende–plagioclase thermometer. Zircon saturation thermometry attests to a near-liquidus temperature range from 794 to 853 °C.

Partial corrosion of magmatic epidote in these four plutons occurred during an interval of no more than 10–30 years, which corresponds to maximum magma ascent rates of 650–1000 m/year. Diking, associated with regional shearing, probably facilitated rapid transport of granitic magma through hot continental crust at peak metamorphism, and permitted survival of epidote that was out of equilibrium at the low pressure of final emplacement. Similarities between mineralogical composition, chemistry, and isotopic compositions ($\varepsilon Nd_{(0.60Ga)}$ between −2 and −5, T_{DM} from 1.2 to 1.3 Ga, $\delta^{18}O$ values>10‰, V-SMOW) of these four plutons and Neoproterozoic magmatic epidote-bearing plutons elsewhere in northeastern Brazil, argue for similar metabasaltic/mafic sources that had previously experienced low-temperature alteration.

1. Introduction

The chemical and mineral compositions of magmatic rocks are combined outcome of the chemical composition of the source, nature of the processes of melt segregation, ascent and emplacement, and accompanying mineral fractionation and wall-rock assimilation. Detailed geochemical studies provide insight into these source attributes and subsequent magmatic processes, and the tectonic environment. Chemical compositions of amphibole, feldspar, biotite, epidote, titanite, and Fe–Ti oxide minerals reflect physicochemical parameters (pressure, temperature, and oxygen fugacity) during crystallization (e.g., Abbott, 1985; Abbott and Clarke, 1979; Speer, 1987). Al-in-hornblende is considered to be a reliable barometer (e.g., Anderson and Smith, 1995; Hammarstrom and Zen, 1986; Schmidt, 1992) and the hornblende–plagioclase pair is considered to be a reliable thermometer (Blundy and Holland, 1990; Holland and Blundy, 1994), provided that assumptions are fulfilled upon which these methods are based. Magmatic epidote (mEp) can be also used for estimating pressure and oxygen fugacity during magma crystallization (e.g., Naney, 1983; Zen and Hammarstrom, 1984). Titanite composition, being P–T dependent (Enami et al., 1993) has also been employed, in conjunction with Fe–Ti oxide compositions, to estimate oxygen fugacity (Wones, 1989).

High-K calc-alkalic granitoids have high-K contents and are enriched in other incompatible elements (e.g. U, Th, Rb and some rare earth elements) compared to low-K calc-alkalic granitoids. High-K I-type granitoids, although prominent features of orogenic belts, are surprisingly the least understood granitoids in terms of processes and source materials (Roberts and Clemens, 1993) despite the use of trace element geochemistry, isotope systematics and experimental petrology. Uncommon chemical characteristics have attracted attention to high-K calc-alkalic granitoids (e.g. Ague, 1987; Speer, 1987; Vyhnal et al., 1991). Empirical thermodynamic calculations have been applied to chemical compositions of mineral pairs of calc-alkalic and high-K calc-alkalic plutons and results together with bulk rock chemistry, help to classify them, work out their crystallization history and gain a better understanding of their tectonic meaning.

* Corresponding author.
E-mail address: sial@ufpe.br (A.N. Sial).
[1] Current address: Companhia de Pesquisa de Recursos Minerais, Av. Sul 2291, Afogados, Recife, PE, 50770-0, Brazil.

0024-4937/$ – see front matter © 2011 Elsevier B.V. All rights reserved.
doi:10.1016/j.lithos.2011.09.017

The Borborema Province, in northeastern Brazil, covers an area of about 380,000 km^2, developed during the Brasiliano Cycle (Almeida et al., 1981). It is limited by the São Francisco and Parnaíba provinces as well as by coastal basins and part of the continental margin. Geochemical and isotopic (U–Pb zircon; whole-rock Sm–Nd) studies have helped to subdivide the Borborema Province into different tectonic domains (e.g., Almeida et al., 1981; Fetter et al., 2000; Hackspacker et al., 1990; Van Schmus et al., 1995 among others). Neoproterozoic plutonic magmatism in this province consists of several associations (Ferreira et al., 1998, 2004; Sial, 1986; Sial et al., 2008), of which the high-K calc-alkalic (with a minor magmatic epidote-bearing component) rocks are the most voluminous. Plutons in this association intrude different tectonostratigraphic terranes of the Borborema Province.

Notable characteristics of Borborema high-K calc-alkalic granitoids include well-preserved internal structures (e.g., Tavares pluton; Weinberg et al., 2001), their emplacement at mid-crustal levels closely related to active shear zones (Weinberg et al., 2004), and their petrology (e.g., Ferreira et al., 2004, 2011; Sial, 1986; Sial et al., 1999, 2008).

In an effort to further understand these intriguing plutons, we selected four of them (Conceição das Creoulas, Caldeirão Encantado, Murici, and Boqueirão) to gain insight through mineral chemistry into the P–T conditions at which they formed and crystallized. Additionally, we examined their Nd and O isotope compositions, and attempted to estimate their rates of upward magma transport. These plutons are exposed along the southwestern margin of the NE–SW trending Alto Pajeú terrane, which is one of the many terranes comprising the Borborema Province (Fig. 1).

2. Geologic setting and petrography

Accretion of tectonostratigraphic terranes is a plausible model for the development of the Borborema Province (e.g., Brito Neves et al., 1995, 2000; dos Santos and Medeiros, 1999; dos Santos et al., 1995, 1997, 2010; Rodrigues and Brito Neves, 2008). Mafic to ultramafic complexes, some of them interpreted as remnants of oceanic crust (Beurlen et al., 1992) occur near suspect terrane boundaries, and were used by dos Santos et al. (1997) as evidence for the collision of continental blocks. Other authors present an alternative hypothesis, based on geochemical signatures of high-K calc-alkalic and associated dioritic rocks (e.g. Mariano et al., 2001, 2009; Neves et al., 2000, 2009), as well as on the absence of ophiolites or other indicators of a continental margin, to argue for an intracontinental origin for the province (e.g., Neves, 2000).

The Alto Pajeú terrane, which is composed of a metavolcano-sedimentary sequence, experienced peak metamorphism during the 960 Ma contractional Cariris Velhos event (dos Santos et al., 2003). According to Ferreira et al. (2004), this terrane was reworked during the late Neoproterozoic and it was characterized by intense granitic activity in three time intervals beginning with emplacement of magmatic-epidote bearing high-K calc-alkalic, calc-alkalic, and shoshonitic magmas during the 650–620 Ma interval (Ferreira et al., 2004; Ferreira et al., 2011; Sial et al., 2008). The second time interval (590–570 Ma) is marked by abundant intrusions of magmatic epidote-free high-K calc-alkalic magmas, followed by unique ultrapotassic magmas (e.g., Triunfo pluton; Ferreira et al., 1994). The final interval (545–520 Ma), characterized by peralkaline granitoids and rare A-type magmas, marked the end of the Brasiliano cycle in this region (da Silva Filho et al., 1993; Ferreira and Sial, 1997).

The Conceição das Creoulas pluton is located between two northeast-trending sinistral shear zones. The pluton, covering approximately 120 km^2 (#1, Fig. 1), has an elliptical outcrop pattern and its ENE-trending greater axis lies in an angular relationship with the regional tectonic fabric (NE–SW) of the Alto Pajeú terrane. This pluton is weakly deformed in its interior, but solid-state deformation increases toward its margins where quartz is recrystallized and myrmekite developed. This pluton is intrusive into the Mesoproterozoic Riacho do Forno/Recanto Formation gneiss–migmatite basement (dos Santos, 2000). The wall-rock foliation is concordant with the semi-elliptical shape of the pluton, and its internal foliation has gentle dips (<40°) at the margins, becoming gentler or nonexistent toward the core. Foliation is generally concordant with the pluton shape, consistent with a forceful expansion of the pluton.

The Caldeirão Encantado pluton forms a very peculiar structure (# 2, Fig. 1), consisting of a set of high-K calc-alkalic granodiorite sheets. These sheets have intruded gneisses and quartzites of the basement,

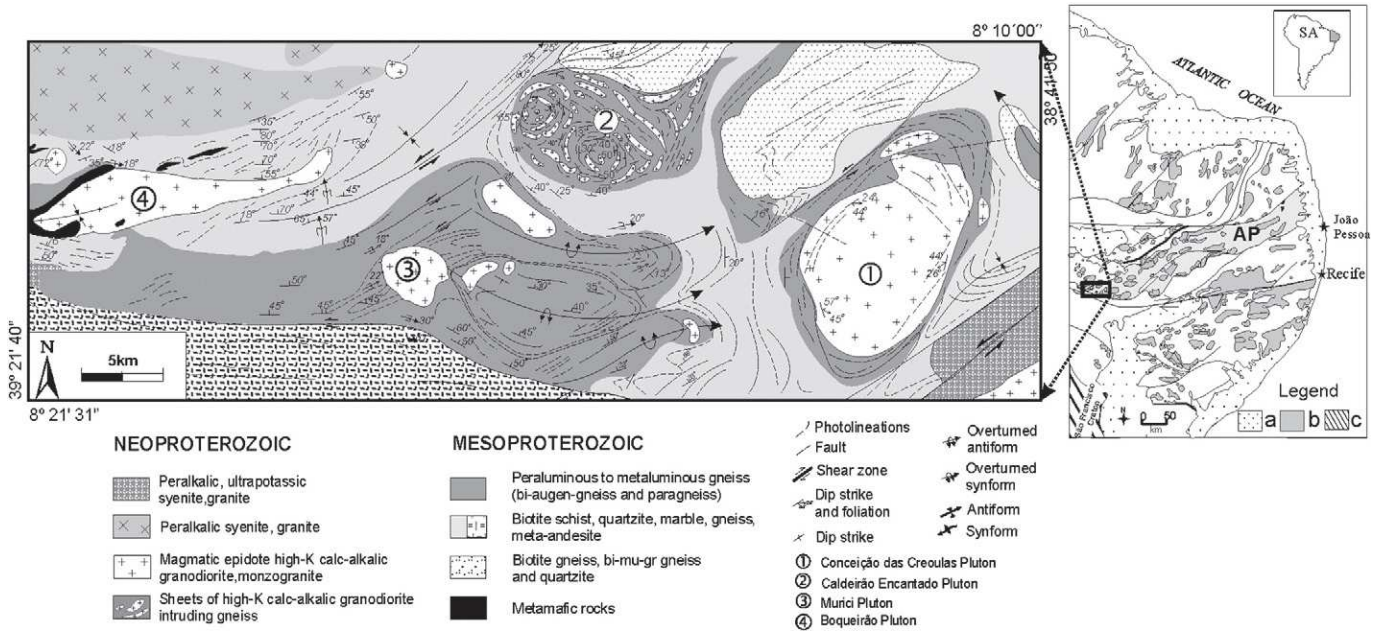

Fig. 1. Geologic map of the study area showing distribution of the studied plutons (numbered 1 through 4) within the Alto Pajeú terrane, Neoproterozoic Borborema Province, northeastern Brazil. In the index map to the right, rectangle outlines the study area: (a) Phanerozoic undeformed sedimentary cover, (b) granitoids and syenitoids and (c) São Francisco Craton, (AP) Alto Pajeú terrane.
Modified from Ferreira et al. (1998, 2004) and Brito Neves et al. (2003).

determining two "bull's-eye" substructures in plan view. Within these substructures, granitic sheets dip inward in an arrangement somewhat similar to cone-sheet structures. This pluton, also emplaced into Mesoproterozoic gneiss/migmatite of the Riacho do Forno/Recanto Formations (dos Santos, 2000), is located near a sinistral shear zone.

The strongly deformed Murici pluton is approximately circular (# 3, Fig. 1) and was emplaced into Mesoproterozoic gneisses. Its solid-state deformation increases toward the margins, where granites have recrystallized quartz grains, myrmekite, and K-feldspar crystals with recrystallized tails (as a result of solid-state deformation of zoned K-feldspar megacrysts).

The Boqueirão pluton is about 45 km long in an ENE direction, parallel to the Serra do Boi Morto sinistral shear zone, and located close to the boundary between the Alto Pajeú and Cachoeirinha–Salgueiro terranes (# 4, Fig. 1). This pluton intrudes along the major contact between Mesoproterozoic gneisses (both fine-grained and augen) of the Recanto/Riacho do Forno Formation, and biotite schists of the Riacho da Barreira Complex (dos Santos, 2000). Its western portion intrudes Paleoproterozoic gneisses and amphibole schists. In this internally homogeneous pluton, the magmatic/solid state foliation has relatively high dips (>40°) that are parallel to foliation of the host rock. Xenoliths of schist commonly are elongate parallel to the rock's foliation.

All of these plutons are characterized by extraordinary magmatic and solid-state structures (examples shown in Fig. 2): (a) mafic-rich layers generally aligned parallel to the regional foliation, with a few curved semi-circular schlieren, (b) irregular distribution of megacrystic aggregates, (c) incipient ladder dikes similar to those reported by Weinberg et al. (2001) for the Tavares pluton (a similar pluton in this Province), and (d) recrystallized tails resulting from solid-state deformation of zoned K-feldspar megacrysts in the Murici pluton. Ladder dikes are characterized by concave mafic-rich layers with biotite and epidote as main mineral components (Sial et al., 2008) that alternate with felsic-rich layers having a mineral composition similar to the host granite and, in a number of cases, K-feldspar aggregates that in cross section occupy the nucleus of concentric ellipsoids in horizontal exposures. The K-feldspar aggregates are 10 cm to a few meters in size. According to Weinberg et al. (2001) this type of feature results from convective currents set up by the underplating of mafic magma which creates a temperature contrast within the magma chamber.

These plutons are petrographically and mineralogically similar, and comprise coarse porphyritic granodiorites and monzogranites (Fig. 3). However, they show extreme variations in the ratio of K-feldspar megacrysts to groundmass, even at outcrop scale. The groundmass texture is mostly medium- to coarse-grained, comprised of quartz, K-feldspar, and plagioclase as the main mineral phases, with minor biotite and hornblende, and trace abundances of epidote, titanite, allanite, apatite, zircon, and Fe–Ti oxides.

K-feldspar megacrysts are coarse perthitic microcline, up to 8 cm long, typically displaying Carlsbad twinning, possibly overprinted by cross-hatched twinning, suggesting orthoclase–microcline inversion that was incomplete on account of prevalent low water pressure during crystallization. Their megascopic shape is rectangular and subhedral, but microscopically they have rounded corners and irregular edges that are rimmed by anhedral intergrowth of very fine-grained plagioclase, microcline, quartz, biotite, hornblende, and myrmekite. Most K-feldspar megacrysts exhibit megascopic oscillatory zoning and oriented inclusions of plagioclase near the core, in addition to inclusions of biotite, titanite, hornblende, and epidote.

Less abundant plagioclase megacrysts are smaller (2 to 0.5 cm), comprising the major feldspar in the groundmass. The larger plagioclase grains commonly contain minor inclusions of hornblende, biotite, and epidote. Some crystals show weak oscillatory zoning with slightly less sodic rim compositions, and with variable degrees of sericitization. Anhedral quartz grains, with inclusions of hornblende, have characteristic undulatory extinction and are intergrown with feldspar. Hornblende occurs as subhedral crystals (0.2 to 5 mm) and as small inclusions in quartz and feldspar. Some twinned hornblende grains are also observed. Long axes of glomerocrysts are commonly aligned parallel to flow foliation of the host granitoids. Dark green biotite is the most abundant mafic mineral (up to 10 vol.%), occurring as flakes filling interstitial spaces and as anhedral to subhedral glomerocrysts with large variation in size (0.5 to 30 mm) and generally aligned parallel to the foliation. Apatite, hornblende, epidote, titanite, and zircon are common inclusions in biotite.

Epidote is the most abundant accessory phase (ranging from 1.5 to 5 modal%) and it occurs in a number of textural relationships resembling those in magmatic epidote-bearing plutons elsewhere in the Borborema Province described by Sial et al. (2008): (a) as euhedral to subhedral crystals with allanite cores, included in biotite, some

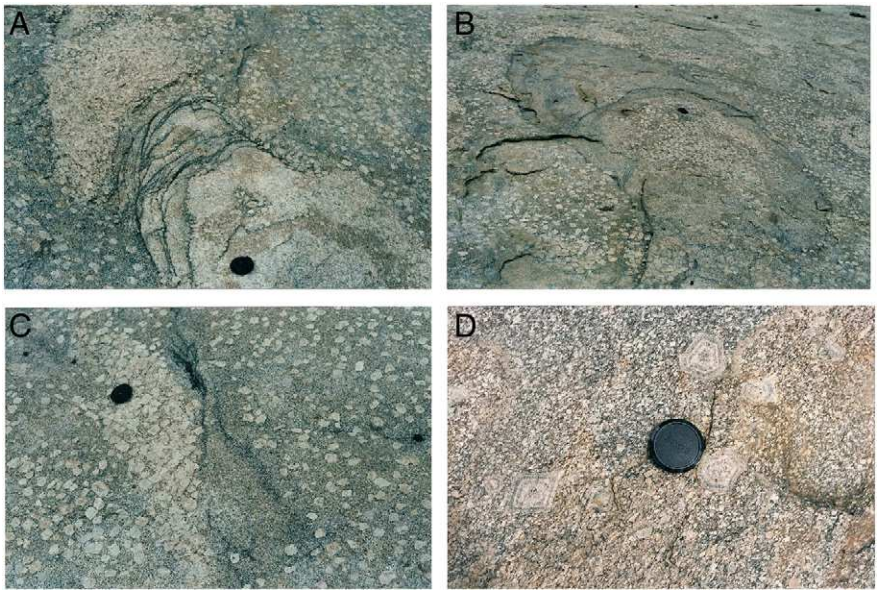

Fig. 2. Magmatic and solid-state structures: (A) incipient ladder dike, exhibiting K-feldspar cumulates in its upper end; Conceição das Creoulas pluton; (B) magma differentiate as a result of filter pressure in the Conceição das Creoulas pluton; (C) irregular distribution of crystal aggregates, a common feature in all four studied plutons; (D) recrystallized tails as a result of solid-state deformation of oscillatorily zoned K-feldspar megacrysts in the Murici pluton.

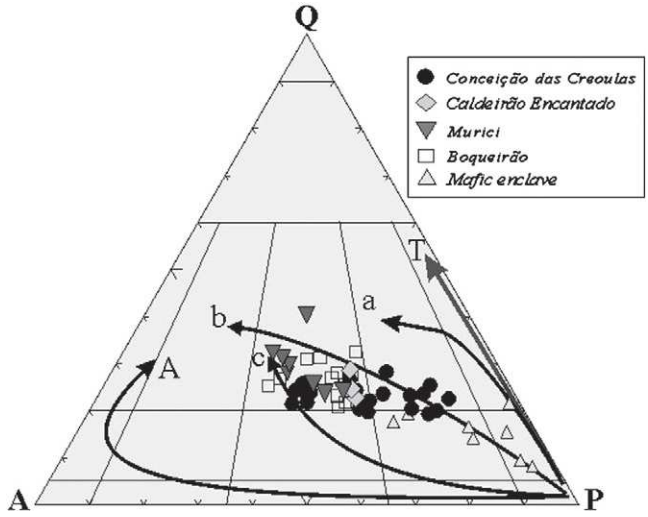

Fig. 3. QAP modal diagram for the studied plutons (Streckeisen, 1976). Trends from Lameyre and Bowden (1982): T—tholeiitic series; A—alkalic series; calc-alkalic series: (a) low K calc-alkalic, (b) medium K calc-alkalic, (c) high K calc-alkalic.

with partly resorbed margins in contact with felsic minerals. In a few cases, allanite cores also display twining and compositional zoning (Fig. 4A) ('type a' epidote); (b) as allanite-free, euhedral to subhedral grains occurring as inclusions within biotite (Fig. 4B) ('type b' epidote); (c) as partly embayed subhedral grains within plagioclase laths (Fig. 4C), and relatively smaller compared to epidote grains associated with biotite ('type c' epidote); (d) as a late-crystallized phase, observed in intergranular spaces between plagioclase, biotite, and hornblende ('type d' epidote); (Fig. 4D). In a few cases, biotite and hornblende are seen as inclusions in epidote.

Distinctive textural attributes of epidote grains such as: (a) euhedral to subhedral habit, (b) twinning and strong compositional zonation, (c) allanite-rich cores; (d) crystallization after hornblende but before or contemporaneous with biotite, (e) in some cases embayed where in contact with the feldspar crystals, and (e) the lack of biotite alteration to chlorite and fresh appearance of plagioclase, are diagnostic of their magmatic origin.

Titanite occurs as slightly pleochroic subhedral crystals, up to a few millimeters long, present in feldspar, along margins of hornblende and biotite crystals or as euhedral grains in the groundmass, and as zoned and secondary fine-grained crystals associated with biotite. Apatite occurs as slightly elongated euhedral crystals (0.05 to 0.15 mm) included in hornblende and biotite, or as an early-crystallized phase. Fe–Ti oxide minerals are rare, occurring as minute grains within or adjacent to biotite and titanite, except in the Murici pluton where they occur as large euhedral to subhedral magnetite crystals.

Microgranitoid mafic enclaves (quartz diorite to quartz monzodiorite) of a variety of sizes and shapes are common throughout these four plutons and the mineralogical composition of the enclaves is essentially the same as the host granitoids, but with greater modal abundance of biotite and amphibole.

3. Age, neodymium, and oxygen isotopes

A Neoproterozoic age for the Conceição das Creoulas pluton (the only one dated among the four studied plutons) has been established by a whole-rock Rb–Sr isochron (5 samples) analyzed at the Federal University of Pará, Belem, Brazil. The determined age and initial ratio are $t = 638 \pm 29$ Ma, $Sr_0 = 0.7093 \pm 0.004$, MSWD = 4.96 (Brasilino et al., 1999).

Sm–Nd analyses were made of 9 whole-rock samples at the Geochronological Laboratory, University of Brasilia, Brazil, by conventional cation exchange techniques using Teflon columns containing LN-Spec resin (HDEHP—diethylhexyl phosphoric acid supported on PTFE powder). Sm and Nd were loaded on Re evaporation filaments of double filament assemblies, and the isotopic measurements were carried out on a multi-collector Finnigan MAT 262 mass spectrometer in static mode. Uncertainties for Sm/Nd and $^{143}Nd/^{144}Nd$ ratios are better than ±0.4% (1σ) and ±0.005% (1σ) respectively, based on repeated analyses of international rock standards BHVO-1 and BCR-1. $^{143}Nd/^{144}Nd$ ratios were normalized to $^{146}Nd/^{144}Nd$ of 0.7219, and the decay constant used was 6.54×10^{-12} a^{-1}.

Model ages are within the 1.2–1.5 Ga (T_{DM}) interval, and εNd (at 0.60 Ga) ranges from values in the −2.0 to −2.6 interval (Conceição das Creoulas pluton) to values in the −4.1 to −5.0 interval (Boqueirão, Caldeirão Encantado, and Murici plutons). Five samples from the

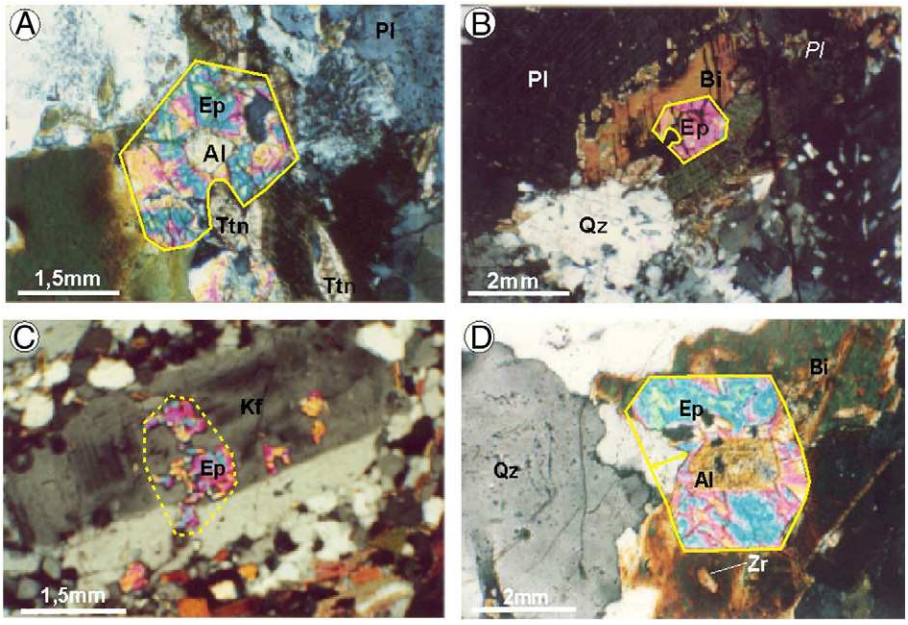

Fig. 4. Textural attributes of magmatic epidote: (A) euhedral magmatic epidote with allanite core; (B) subhedral magmatic epidote in biotite; (C) partly embayed subhedral magmatic epidote enclosed in plagioclase; (D) subhedral magmatic epidote partly enclosed in biotite, showing resorbed margins in contact with the melt.

Conceição das Creoulas pluton yield T_{DM} values in a narrow range of 1.28 to 1.34 Ga (Table 1).

Values of εNd (at 0.60 Ga) and T_{DM} obtained for the Conceição das Creoulas pluton are similar to those observed in calc-alkalic and high-K calc-alkalic magmatic epidote-bearing plutons elsewhere, described by Sial et al. (1999) and by Ferreira et al. (2011). Disparity of εNd (0.60 Ga) for this pluton (−2.0 to −2.6) relative to the other three plutons (−4.1 to −5.0) implies different sources, or similar sources but with different proportions of the same end-members.

For oxygen isotopic analysis, we concentrated zircon, titanite, epidote, and quartz from several kilograms of sample using standard procedures including initial crushing, gold panning, sieving (300 μm meshes), heavy liquid, and Frantz magnetic separations. Final hand picking under a binocular microscope ensured purity of mineral separates. Zircon separates were cleaned in cold hydrofluoric acid followed by cold sulfuric acid. Only the least magnetic fraction of zircon was analyzed. Oxygen isotope compositions of 1–2 mg mineral separates (2–3 mg for zircon) and whole rocks were analyzed by laser fluorination at the Stable Isotope Laboratory (LABISE) of the Federal University of Pernambuco, Brazil, using a CO_2 laser-based high-vacuum extraction line and BrF_5 as the major reagent. Oxygen (gas) released from the reaction between the silicates and BrF_5 was converted to CO_2 at 800 °C. Isotope ratios were determined with a dual inlet, triple collector Thermofinnigan Delta V Advantage mass spectrometer. Results are reported as ‰ deviation with reference to V-SMOW (Table 2).

The values of $\delta^{18}O$ for the mineral separates in these plutons vary little from sample to sample, and are in the expected order for equilibrium, i.e. $\delta^{18}O$ titanite<epidote<zircon<quartz, and this suggests internal isotopic equilibrium in these plutons.

Zircon, the mineral phase that better preserves the original oxygen isotope signatures, yielded high $\delta^{18}O$ values between +9.2 and +9.8‰, V-SMOW. This pattern is observed in magmatic epidote-bearing granitoids elsewhere (Ferreira et al., 2003, Ferreira et al., 2011). According to the Valley et al. (1994) or Lackey et al. (2008) equations to estimate $\delta^{18}O$ for the host magma based on zircon $\delta^{18}O$ and corresponding SiO_2 of the same rock, it implies $\delta^{18}O$ values >10‰ for the host magmas. Whole-rock $\delta^{18}O$ values (relative to V-SMOW) are all above +10‰, V-SMOW as well and for quartz, $\delta^{18}O$>+12.5‰ (Table 2). For comparison, the table shows similar high $\delta^{18}O$ values for quartz and whole rock in the calc-alkalic, magmatic epidote-bearing Pedra Branca and Boa Ventura plutons in the Cachoeirinha–Salgueiro terrane.

The high $\delta^{18}O$ values, and low magnetic susceptibility (average< 0.5×10^{-4} SI), are consistent with a metasedimentary source ($\delta^{18}O$> 10‰; O'Neil et al., 1977). However, these granitoids are not typical S-type as observed by Ishihara (1977) and Takahashi et al. (1980), but rather, the mineralogy comprised of hornblende, titanite, and biotite, favors an I-type source for their parental magmas. Fe^{+3} is tied up in epidote, and not in iron oxide minerals, which explains the observed low magnetic susceptibility.

Table 1
Sm-Nd data for the four plutons.

Pluton	Sample	$^{147}Sm/^{144}Nd$	$^{143}Nd/^{144}Nd$	εNd (0.60 Ga)	εNd(0)	T_{DM} (Ga)
Conceição das	CC-33	0.113	0.512153	−2.64	−9.46	1.34
Creoulas	CC-26	0.105	0.51213	−2.43	−9.29	1.28
	CC-16	0.113	0.512159	−2.52	−9.34	1.33
	CC-07	0.112	0.512167	−2.28	−9.19	1.31
	CC-27	0.11	0.512172	−2.02	−9.09	1.28
Caldeirão	CALEN S	0.1167	0.512067	−5.01	−11.14	1.51
Encantado	CALEN34	0.0994	0.511966	−5.65	−13.12	1.42
Murici	PM2	0.1159	0.512085	−4.60	−10.78	1.47
Boqueirão	BQ4	0.0970	0.512035	−4.12	−11.76	1.31

The high $\delta^{18}O$ values for these magmas can be explained by the participation of a volumetrically important metabasaltic/mafic rock in the source that has undergone low-temperature interaction with water. This mechanism is similar to what happens in the ocean where hydrothermal alteration of seafloor basalts leads to high $\delta^{18}O$ without disturbing the original Nd-isotope signature (Muehlenbachs et al., 1986).

4. Bulk rock chemistry

Major and trace element analyses were carried out by X-ray fluorescence (1 mg of sample/5 mg of lithium tetraborate fused bead, and Kα radiation in a RIX-3000 Rigaku XRF unit), in the Department of Geology of the Federal University of Pernambuco. Some additional trace elements and REE were analyzed by inductively coupled plasma (ICP) spectrometry at the Geosol-Lakefield Laboratory, Minas Gerais, after being concentrated through ion-exchange chromatography. (Major, trace, and REE analyses referred to in the text are found in Supplemental electronic data Tables 1 through 3, Appendix A, in the online version).

The major element chemistry is characterized by an SiO_2 range of 65–75%, alkali contents around 6.5%, MgO varying from 0.91 to 1.8%, and CaO from 2.4 to 3.5%. The rocks are high-K calc-alkalic, metaluminous to slightly peraluminous, with most samples showing minor normative corundum. These rocks are enriched in Ba (650–1737 ppm) and Sr (500–1737 ppm), and have moderate Rb (87–147 ppm). The Zr content ranges between 189 and 345 ppm, while Nb is relatively low (<20 ppm).

Negative correlations of SiO_2 with TiO_2, CaO, MgO, MnO, Fe_2O_3 and P_2O_5 are observed. The alkalis (Na_2O and K_2O) show a positive correlation with SiO_2, while Al_2O_3 does not show any systematic variation. Such major element trends point to fractional crystallization as the important petrogenetic process, further supported by some trace element patterns such as positive correlations between Ba/Rb vs. Zr/Rb, and Zr/Rb vs. Sr/Rb (Fig. 5A).

The ORG-normalized incompatible elements pattern (a spidergram, not shown) is characterized by high LILE/HFSE ratios. ΣREE ranges from 119 to 247 ppm (except for the Murici pluton, which has a lower range: 80–94 ppm). The REE patterns indicate enrichment in LREE relative to HREE (Fig. 5B), indicating significant fractionation (La_n/Lu_n = 40–60), except for the Murici pluton, which has La_n/Lu_n (91–94), attesting that fractionation in this pluton was less effective. Eu anomalies are minor to absent and suggest that either feldspar fractionation was insignificant, or that fO_2 was relatively high during magma crystallization.

5. Mineral chemistry

Feldspar, amphibole, biotite, epidote, titanite, and apatite were analyzed by electron microprobe: JEOL JXA-8600 (University of São Paulo, Brazil) and CAMECA SX50 (University of Brasilia, Brazil). The operating conditions were maintained at 15 kv, 10 μA with beam exposure time of 6 s, applying ZAF correction. Chemical compositions and structural formulas are listed in Supplemental electronic data Tables 1 through 5, in Appendix B. The mineral analyses have been recalculated into mineral formulas and cationic proportions using MINFILE for DOS (Afifi and Essene, 1988), MINPET for WINDOWS (Richard, 1995), AMPHICAL (Yavuz, 1998), and LIMICA (Yavuz, 2001).

5.1. Feldspar

Plagioclase compositions (Supplemental electronic data Table 1, Appendix B) range between An_{21-30} (oligoclase–andesine) for the Conceição das Creoulas pluton and An_{18-30} (oligoclase–andesine) for the Caldeirão Encantado, Boqueirão, and Murici plutons (Fig. 6).

Table 2
Oxygen isotope data (V-SMOW ‰) for whole-rock and mineral separates from the four plutons.

Pluton	Zircon	Quartz	Epidote	Titanite	Feldspar	w.r.	zirc-tit	qz-epid	qz-zir	qz-tit	zirc-epid	qz-feld	epi-tnt	SiO_2	Zr	calc. w.r.
Conceição das Creoulas																
CC		13.85	9.16	8.86		12.07		4.69		4.99			0.30			
RCC-02	9.73	13.78	8.47	8.72			1.01	5.31	4.05	5.06	1.26		−0.25	70.4	232	11.63
RCC-3a		14.29				11.69										
RCC-4		13.36	9.35	8.72				4.01		4.64			0.63	66.1	234	
RCC-5		13.77	9.56	8.63				4.21		5.14			0.93	66.9	275	
RCC4/5	8.83															
Caldeirão Encantado																
CALEN-V		13.10	8.65	8.35	11.68	11.3		4.45		4.75		1.42	0.3			
CALEN-11		13.46	9.24	8.1		11.6		4.22		5.36			1.14	68.84	247	
CALEN 34	9.74		8.83	8.4		10.9	1.34				0.91		0.43			
Scalen-v		13.37	8.88	8.57		10.91		4.49		4.8			0.31			
Murici																
PM-1	9.29	12.83	8.55	7.59		10.6	1.7	4.28	3.54	5.24	0.74		0.96	63.69	210	10.80
PM-2	9.16	13.01	8.99	7.78		10.8	1.38	4.02	3.85	5.23	0.17		1.21	63.11	193	10.64
PM-3	9.26	12.55	7.64	7.50		10.5	1.76	4.91	3.29	5.05	1.52		0.14	63.06	292	10.74
PM-10	9.34	12.95	9.00	7.64			1.7	3.95	3.61	5.31	0.34		1.36	62.96	218	10.81
PM-11														69.86	284	10.59
Boqueirão																
BQ-4				8.37												
BQ-9	9.31	13.06	9.28	7.98			1.33	3.78	3.75	5.08	0.03		1.30	64.31	189	10.86
BQ-13		13.58	9.03	8.35				4.55		5.23			0.68	68.98	239	
BQ-15	9.54	13.23	8.98	8.32			1.22	4.25	3.69	4.91	0.56		0.66	65.27	291	11.15
Pedra Branca																
PB-1		12.20				11.56										
PB-2		11.82				11.80										
PB-3		12.65				11.84										
Boa Ventura																
BV-1		11.97				11.62										
BV-2		12.79				11.30										
BV-3		12.59				10.12										

They show mild reverse zoning with the core slightly enriched in Na. Microprobe analyses of K-feldspar indicate that the proportion of albite component in solid solution is in the range of 6–9%, and a composition range within Or_{89}–Or_{93} for the Conceição das Creoulas, Or_{90}–Or_{94} for the Boqueirão, and Or_{91}–Or_{98} for the Caldeirão Encantado and Murici plutons, with a gradual increase in albite molecule toward the rim.

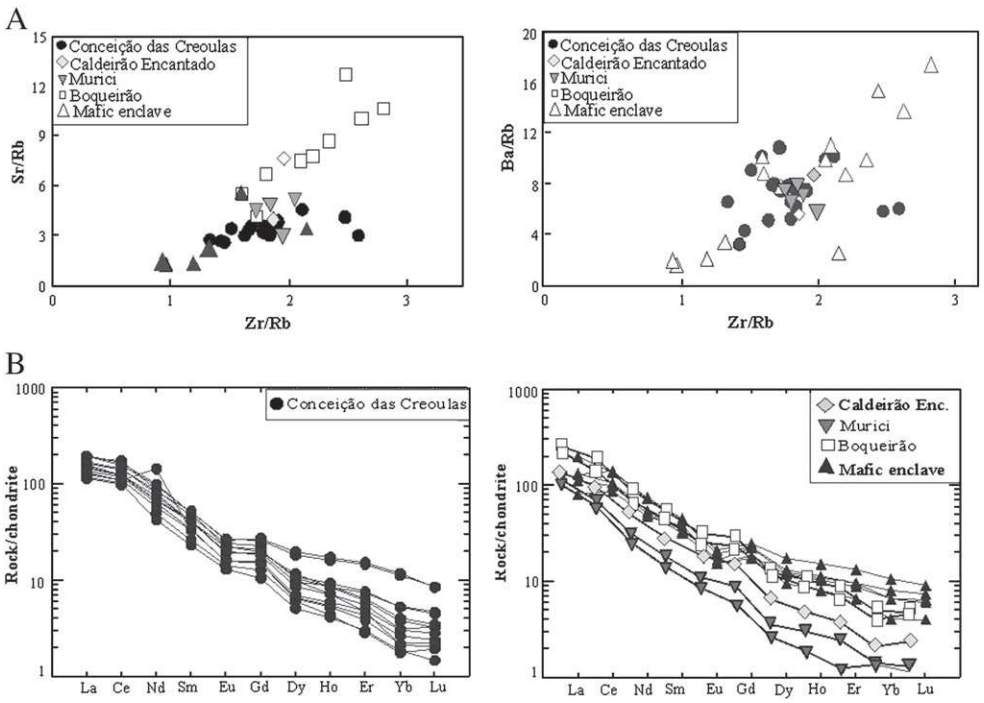

Fig. 5. (A) Ba/Rb vs. Zr/Rb, and Zr/Rb vs. Sr/Rb diagrams, for the studied plutons; (B) chondrite-normalized REE patterns for representative samples from the studied plutons.

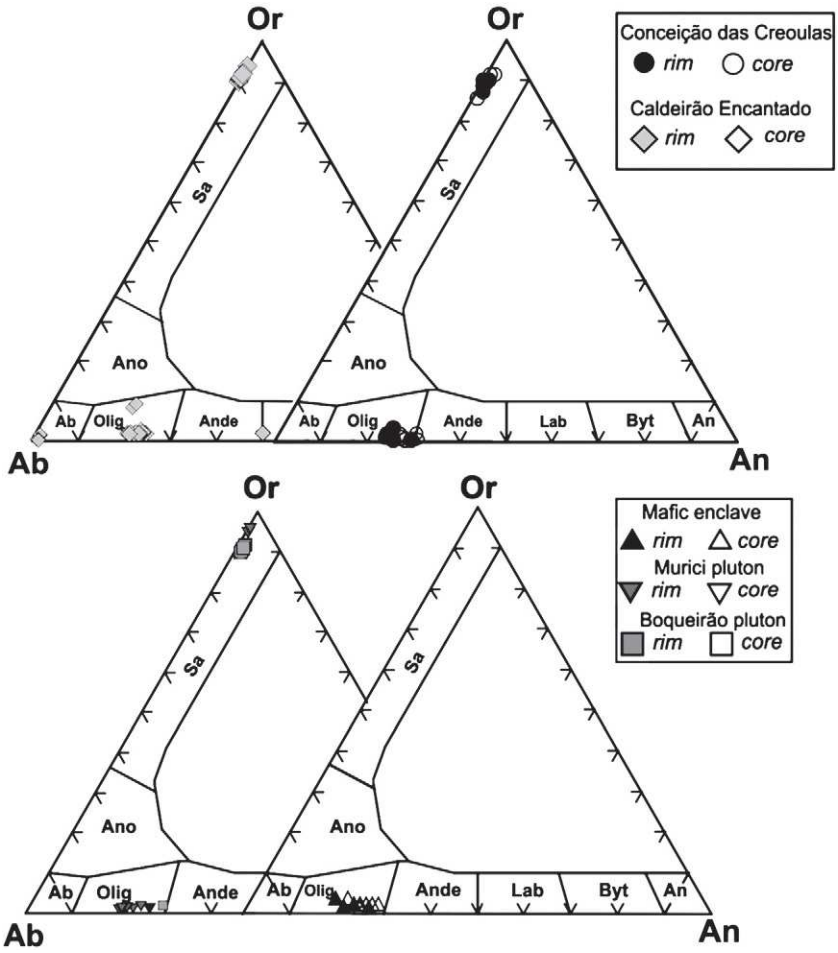

Fig. 6. Classification of the feldspars from the studied plutons.

5.2. Hornblende

Analyses of amphibole in the porphyritic granitoids and mafic enclaves (Supplemental electronic data Table 2, Appendix B) classify them as calcic amphiboles according to the scheme of Leake (1978). Hornblende in the porphyritic granitoids and enclaves is edenite to ferropargasite, very close to the field of ferro-edenite, whereas hornblende data from Boqueirão plot in the ferroedenite to ferro-tschermakite fields (Fig. 7). The Mg/(Mg + Fe) ratio (0.40–0.58) is in accordance with the ranges prescribed for calc-alkalic granitoids (Mason, 1985), while the Fe/(Fe + Mg) ratios suggest crystallization of this phase under moderately high fO_2. The Si content varies from 6.3 to 6.5 atoms per formula unit (afu). Fig. 8 illustrates a positive correlation between Al^{IV} and Al^{T} in the amphiboles, similar to that reported by Hammarstrom and Zen (1986).

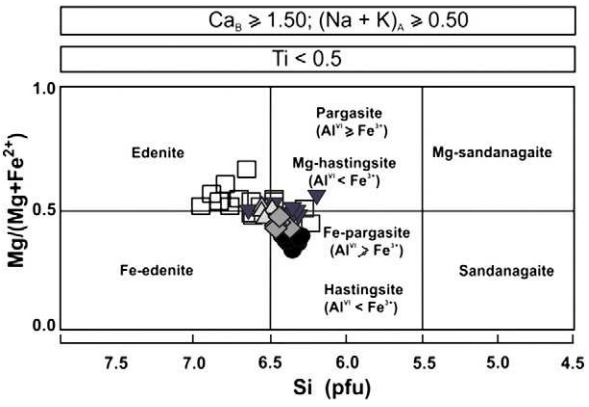

Fig. 7. Classification of amphiboles from the studied plutons (fields after Leake, 1997). Symbols are the same as in Fig. 3.

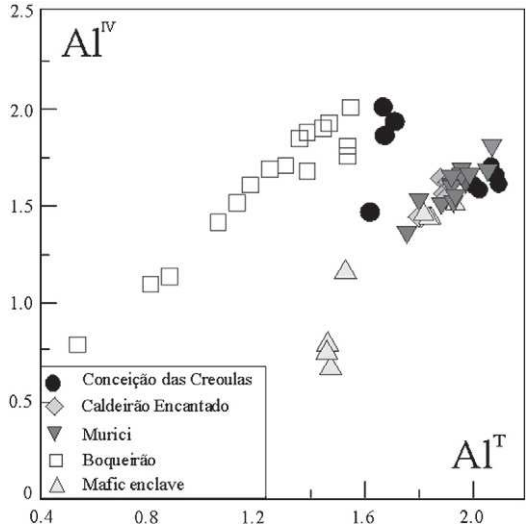

Fig. 8. Relationship between Al^{IV} and Al^{T} in amphiboles from the studied granitoids.

5.3. Biotite

Microprobe analyses of biotite (Supplemental electronic data Table 3, Appendix B) indicate compositions lying approximately midway between phlogopite and annite (Fig. 9). The range of molar Fe/(Fe + Mg) is relatively higher (0.46–0.6), with intermediate Al content. Biotite compositions for porphyritic granitoids and mafic enclaves are similar, and show slightly enriched Mg concentration (8.78–12.2 wt.%) and FeO/MgO ratios between 1.5 and 2.2. Biotite from calc-alkalic granitoids has relatively lower Mg content, with an average FeO/MgO ratio of 1.76, consistent with the ranges reported by Abdel-Rahman (1994). In an MgO vs. Al_2O_3 diagram (Fig. 10A), the biotite compositions plot in the calc-alkalic field, showing a slight tendency toward elevated Al content. Porphyritic granitoids and mafic enclaves show slight negative correlation between Al^T and Mg (Fig. 10B). Nachit et al. (1985) proposed this diagram as a means to identify magmatic series that evolved through distinctive crystal fractionation processes. The alumina saturation index of biotite (ASI, $Al^T/Ca + Na + K$) is significantly low (1.0–1.5), and reflects low alumina activity in the crystallizing magma (Zen, 1988).

5.4. Epidote

Supplemental electronic data Table 4, Appendix B, provides microprobe data of representative mEp grains. mEp grains in the Conceição das Creoulas pluton are typically zoned, with Fe^{+3} contents increasing from core to rim. The pistacite (Ps) content varies systematically from the highest values encountered in epidote with allanite core [type "a" ($Ps_{24–25}$)], followed by those rimmed by biotite [type "b" ($Ps_{21–23}$)] and inclusions in feldspar [type "c" ($Ps_{20–21}$)]. In the Conceição das Creoulas pluton, a limited variation in Ps probably reflects a narrow range of fO_2 in the system. The Ps range of epidotes with allanite cores (around Ps_{25}) is consistent with crystallization along the NNO buffer (Liou, 1973).

Epidote grains in the Caldeirão Encantado and Boqueirão plutons have Ps contents between 22 and 27%, with high values of $Ps_{25–26}$ encountered in epidote with allanite cores in Caldeirão Encantado; Ps contents in the Murici pluton show broader compositional variation ($Ps_{20–29}$). Some of the observed variation in Ps content is related to inclusions in feldspar ($Ps_{21–22}$); mEp rimmed by biotite ($Ps_{22–24}$), epidote with allanite cores ($Ps_{24–26}$), and mEp associated with magnetite ($P_{26–27}$). As a whole, the Ps range for epidotes in all four plutons is consistent with crystallization between the NNO and HM buffers.

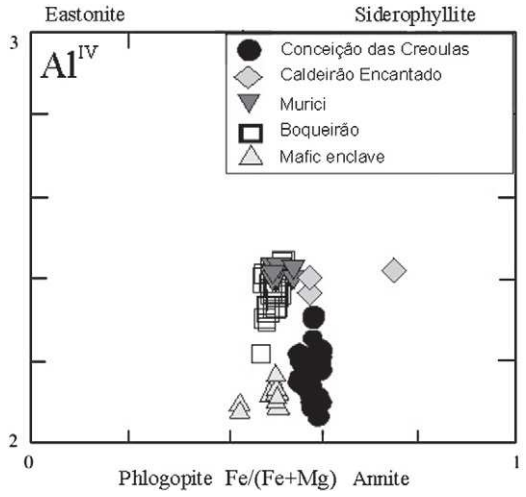

Fig. 9. Al^T vs. Fe/(Fe + Mg) diagram for biotites from the studied granitoids. Symbols are the same as in Fig. 3.

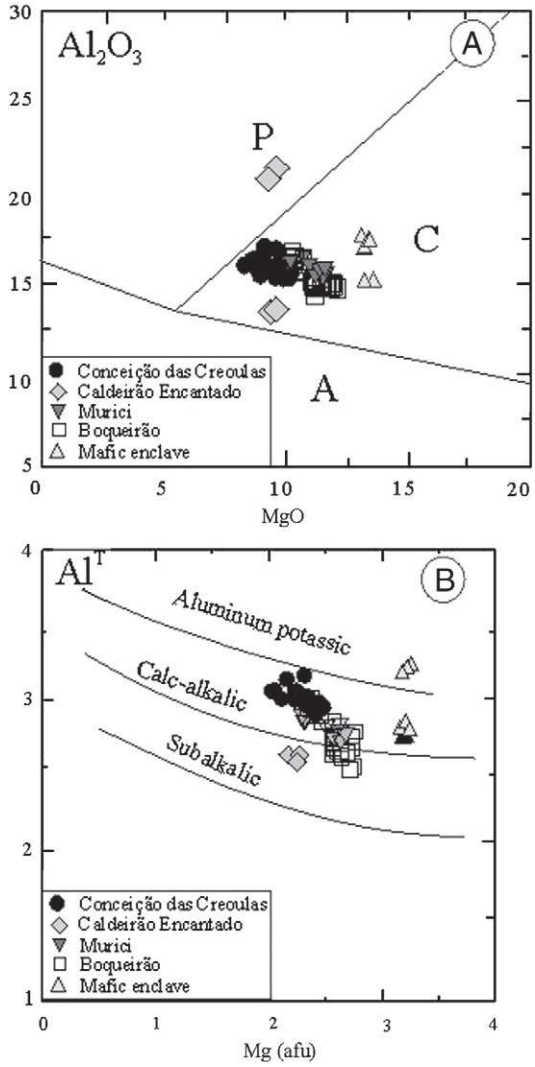

Fig. 10. (A). MgO vs. Al_2O_3 diagram (after Abdel-Rahman, 1994) showing biotite compositions plotting in the calc-alkalic field. A = alkalic, C = calc-alkalic, P = peraluminous. (B) Al^Tvs. Mg diagram for biotite (Nachit et al., 1985) of the studied rocks, emphasizing fractional crystallization as the most important petrogenetic process in development of these rocks.

In these four high-K calc-alkalic plutons, magmatic epidote seems to have survived dissolution attack by the host magma because it was totally armored by biotite or was within interstices of K-feldspar aggregates. These examples suggest that upward transport was sufficiently rapid for epidote to survive dissolution, accompanied by rapid near-solidus growth of K-feldspar.

Schmidt and Thompson (1996), (Fig. 3) demonstrated experimentally that epidote and plagioclase can coexist around 10 kbar in tonalitic magmas. This situation permits one to estimate rates of magma upward movement where partially dissolved epidote is armored by plagioclase, or epidote has grown with near-solidus K-feldspar at pressures estimated from Al-in-hornblende barometry.

We estimated magma transport rates in the present study using the following approach described in detail by Sial et al. (2008):

(1) selection of mEp on the basis of their mol% Ps, consisting of highly corroded subhedral grains that are partially shielded by plagioclase, biotite, or K-feldspar;
(2) inferring original shapes of corroded grains, and measuring the maximum dissolution zone width;

(3) estimating the duration of corrosion by using the minimum apparent diffusion coefficient of 5×10^{-17} m^2 s^{-1} for Si, Al, Ca, and Fe between tonalitic magma and epidote at 750 °C (Brandon et al., 1996) as follows: $dz = [(D_{app}\times t)^{1/2}]$

where

dz width of dissolution zone (m);
D_{app} apparent diffusion coefficient (5×10^{-17} m^2 s^{-1}); and
t time for partial dissolution of epidote (s)

Accordingly,

$$t = dz^2/\left(5x10^{-17}\right);$$

(4) depth of host magma emplacement was inferred from Al-in hornblende barometry;
(5) the rate of magma transport is the ratio of the route length (difference between the emplacement depth and the source depth) to the average time of corrosion of epidote exposed to the host melt. For melt of tonalite composition at water-saturated conditions and *f*O2 buffered by NNO, plagioclase and epidote may coexist from a depth ~10 kbar (Schmidt and Thompson, 1996, Fig. 2). We infer the route length as the difference between 10 kbar and the emplacement depth. Accordingly,

$$T_r = L_r/t$$

where

T_r ascent rate (m/year)
L_r route length $= (10 - P_e).10^4/3$ (m)
P_e pressure of emplacement (kbar)
t time of partial dissolution of epidote (year)

Calculations using this approach can provide only a maximum speed. This is because the calculations assume implicitly that epidote starts reacting with the host magma as pressure drops below 10 kbar and, therefore, assumes the minimum possible time for corrosion of epidote grains.

Table 3 contains estimates, following this approach, for upward transport rates of the magmas that formed these plutons. Magmas in the Caldeirão Encantado and Boqueirão plutons show maximum ascent rates around 1000 m.year^{-1} and for the other two plutons, around 650 m.year^{-1}.

A close examination of this approach finds some limiting assumptions as already pointed out by Sial et al. (2008): (a) determination of the route length of magma transport; consequence of the magnitude of the error brackets on the Al-in-hornblende barometry, typically in the order of ±0.6 kbar, as well as of the appropriateness of the selection of the correct hornblende generation, (b) use of appropriate diffusion coefficients for Ca, Al, Si, and Fe for each magma composition, (c) bias in measuring dissolution zone widths of mEp grains (only subhedral grains are used and anhedral grains ignored), (d) dependency of the apparent width of the dissolution zone upon the orientation of the examined section, and (e) decreasing rate of epidote dissolution (Fig. 2 of Brandon et al., 1996), leading to an underestimate of digestion time.

Despite these uncertainties, the method clearly provides a good general indication of rapid magma ascent. This is primarily due to the very short calculated dissolution times, i.e., they can be increased by two orders of magnitude and still be short. The rapid rate of upward magma movement suggests diking, and not diapirism, as the ascent mechanism.

Table 4
Temperatures for the studied plutons, determined from zircon saturation.

Conceição das Creoulas pluton			Caldeirão Encantado pluton		
Sample	Zr (ppm)	T °C	Sample	Zr (ppm)	T°C
CC-04	234	827	CE5	264	839
CC-07	222	822	CE-6	320	857
CC-29	266	833	CE-7	328	860
CC-28	302	852	CE-8	295	849
CC-09	290	848	CE-9	239	829
CC-05	275	843	CE10	277	843
CC-06	230	826	CE11	247	832
CC-02	232	826	CE13	295	849
CC-21	212	819	CE14	207	816
CC-16A	244	831	CE16	256	836
CC-20	245	832	CE19	290	848
CC-22	269	840	CE24	239	829
CC-24	265	839	CE32	290	848
CC-26	247	832	CE34	296	850
CC-29	248	839	CE41A	333	861
CC-33	267	839	CE9D	422	886
			CE11D	217	820
			CE32D	240	830
			CE-6E	588	921
Murici pluton					
Sample	Zr (ppm)	T °C	Sample	Zr (ppm)	T°C
PM 01	210	817	PM 09	198	812
PM 02	193	809	PM 10	218	821
PM O3	292	848			
Boqueirão pluton			Mafic enclaves		
Sample	Zr (ppm)	T °C	Sample	Zr (ppm)	T°C
BC 01	212	818	CC-5E	279	826
BC 02	282	845	CC-19E	162	812
BC 06	177	795	CC-20E	198	800
BC13	239	829	CC-24E	174	800
BC 14	297	850	CC-32E	174	793
BC 15	291	848	CC-33E	165	801
BC18	264	838	CE11E1	190	808
BC 21	216	820	PM-10E	190	808
BC-22	262	837	BQ-15E	232	826

5.5. Titanite

Titanite is a widespread accessory mineral in both igneous and metamorphic rocks. Evans and Patrick (1987), Franz and Spear (1985)

Table 3
Estimated rates of magma transport based on magmatic epidote partial dissolution for the Conceição das Creoulas, Caldeirão Encantado, Murici and Boqueirão plutons.

Pluton	Ps epidote (mol%)	Average measured dissolution zone width (mm) of epidote—number of measurements (n)	Time taken for partial dissolution (years)[a]	Pressure (kbar) Al-in-hbl A and S	Temperature (°C) H and B	Rate of upward transport (m/year)
Conceição das Creoulas	21 to 24	0.143 (10)	13	6.5 to 8.5	670 to 720	640
Caldeirão Encantado	27 to 29	0.113 (10)	8		670 to 685	1040
Murici	27 to 29	0.143 (7)	13		650 to 700	640
Boqueirão	27 to 29	0.114 (12)	8.3		640 to 670	1000

[a] Apparent diffusion coefficient $= 5\times10^{-17}$ m^2 s^{-1}, A and S = Anderson and Smith (1995); H and B = Holland and Blundy (1994).

and Tropper et al. (2002) showed strong positive correlation between Al and F contents in aluminous titanite at high pressure. Titanites from the studied plutons are compositionally different from typical magmatic titanites in granitoids (Enami et al., 1993) and show intermediate Al content (0.2–0.54 afu, Supplemental electronic data Table 5) but show positive correlations between Al and F, with slight dispersion. This suggests high pressure of crystallization for titanites in these granitoids. Inferences on the temperature of crystallization were also made. According to Enami et al. (1993), titanite composition depends on pressure and temperature: high temperature titanites with $Al + Fe^{3+}$ (afu) < 1.4. In the studied granitoids, titanite has $Al + Fe^{3+}$ (afu) around 0.6, within the range typical for high-temperature titanites, an observation supported by textural relationships which point to early crystallization of this mineral in these rocks.

5.6. Apatite

Apatite contains relatively high F (2.6–5 wt.%, supplemental electronic data Table 5, Appendix B). Argiolas and Baumer (1978), Girault (1966), and Wyllie et al. (1962) demonstrated a relationship between shape of apatite, and pressure and temperature of magma crystallization. According to Girault (1966), euhedral, slightly elongated apatite grains, such as those in the studied plutons, indicate a relatively slow crystallization process (Wyllie et al., 1962). Homogeneous elongate ratios imply a consistency in the physico-chemical parameters during crystallization.

6. Thermobarometric estimates

6.1. Al-in-hornblende barometry

The linear variation of Al content in hornblendes of calc-alkalic granitoids with crystallization pressure/depth has been used in geobarometric estimates (Schmidt, 1992). The empirical barometric equation that was proposed by Hammarstrom and Zen (1983, 1986) has been subjected to refinement and further calibration to increase the precision level to 1 kbar (Hollister et al., 1987; Johnson and Rutherford, 1989). Schmidt (1992) experimentally calibrated the field-based barometric equation of Hammarstrom and Zen (1986), expanding its applicability up to the 13 kbar pressure level, and maximum Al^t up to 3.37 afu and have used that for H_2O saturated melts.

According to Anderson (1996) and Anderson and Smith (1995), temperature, fO_2, and total pressure influence mafic silicate mineral chemistry, but fO_2 is the main controlling factor. They demonstrated that this barometer yields a falsely elevated pressure when applied to low-fO_2 plutons with iron-rich hornblende, even if hornblende is accompanied by the full barometer assemblage. With increasing fO_2, the Fe/(Fe + Mg) ratio for hornblende and biotite markedly decreases, independent of the whole rock Fe/Mg ratio.

Given these limitations, we have applied the correction proposed by Anderson and Smith (1995) only if the mineral assemblage includes quartz, ferromagnesian silicates, euhedral titanite, and magnetite, and Fe/(Fe + Mg) in hornblende is in the 0.40–0.65 range, characteristics of magmas with relatively high oxygen fugacity. The calculated pressures (Table 5) are 7.5–8.0 kbar for the Conceição das Creoulas pluton, 6.0–7.5 kbar for the Caldeirão Encantado, Boqueirão, and Murici plutons, and 6.4 to 7.0 kbar for mafic enclaves.

6.2. Solidus temperature estimates

6.2.1. Hornblende–plagioclase thermometry

The amphibole–plagioclase thermometry proposed by Blundy and Holland (1990) is valid for a temperature range of 500–1000 °C for plagioclase with <7.8 Si afu. The level of uncertainty in these calculations was subsequently reduced from ±75, to ±35 °C (Holland and Blundy, 1994). The bulk of calculated crystallization temperatures for the studied plutons lie between 632 and 778 °C, the highest temperatures being recorded from the Murici and Conceição das Creoulas samples, and the lowest temperatures from the Boqueirão pluton. Enclaves exhibit a temperature range of 670 to 690 °C.

6.3. Liquidus temperature estimates

6.3.1. Zr thermometry

Whole-rock Zr abundances can be used to estimate the crystallization temperature of zircon in Zr-saturated granitic melts (Watson, 1987). Watson and Harrison (1984) showed experimentally that zircon solubility is correlated with SiO_2. This method assumes that the zircon is not inherited from the source and does not represent a cumulate phase, and is based on the fact that zircon is usually the first mineral to crystallize. Zr thermometric estimates are

Table 5
Summary of mineral chemistry and intensive parameters for the studied high-K calc-alkalic plutons.

	Conceição das Creoulas	Caldeirão Encantado	Murici	Boqueirão	Mafic Enclaves
Plagioclase					
$X_{ab} = (Na/Ca + Na + K)$	0.65–0.70	0.71–0.76	0.69–0.63	0.70–0.79	0.69–0.73
Hornblende					
$Xmg = (Mg/Mg + Fe^{2+})$	0.37–0.53	0.40–0.42	0.48–0.53	0.46–0.53	0.48–0.53
Total Al (apfu)	2.19–2.33		1.93–2.12	1.8–2.18	1.96–2.1
Biotite					
$Xmg = (Mg/Mg + Fe)$					
$ASI = (Al^T/Ca + Na + K)$	–	0.23–0.79	0.14–0.89	0.14–1.09	–
Epidote					
Pistacite content ($Fe^{3+}+/Fe^{3+} + Al$)	0.20–0.25	0.24–0.27	0.20–0.28	0.22–0.27	
Titanite					
$Al + Fe^{3+}$	0.20–0.31	0.25–0.27	0.20–0.29	0.21–0.25	0.15–0.29
F (wt.%)	0.5 0–0.61	0.5–1.13	0.16–0.54	0.11–1.04	–
Apatite					
$Al + Fe^{3+}$	–	3.24–3.46	–	3.14–3.45	–
F (wt.%)					
Pressure kbar (Al-in hornblende)	7.5–8.2	6.5	6.5–7.1	5.9–7.4	6.6–7.0
Temperature °C (pl-hornblende pairs)	668–722	673–681	693–778	632–667	645–700
Temperature °C (Zr-saturation)	819–852	829	809–848	795–848	793–826
Oxygen fugacity (log fO_2)	−17.1 to −17.88	−17.4	−14.4 to −17.03	−16.0 to −19.18	−17.4 to −18.7
Depth of emplacement (km)	25–27	21.5	21.5–23.5	20–25	22–23
Viscosity η_m (Pa.s)	1.3×10^4 to 4.4×10^4	2.9×10^4	1.4×10^4 to 3.2×10^4	1.4×10^4 to 4.6×10^4	–

appropriate for deducing the minimum liquidus temperature, which can be expressed as: $\mathbf{T}(°C) = -\mathbf{273} + \mathbf{12900}/[\mathbf{17.8} - \mathbf{ln}(\mathbf{Zr})]$.

Apatite in mafic enclaves closely follows the 880 °C isotherm (Supplemental electronic data Table 5 in Appendix B; Fig. 11). Apatite in granitoids forms clusters that could be interpreted as showing some kind of accumulation as well.

These calculations are important, being that they provide the only evidence of minimum liquidus temperatures that may be comparable to minimum melting temperature.

6.3.2. Apatite thermometry

Watson (1980) quantified the conditions under which apatite can precipitate in common magma types, and has shown that temperature and silica content of the magma are critical in determining the P_2O_5 content in the magma required for apatite to crystallize. Green and Watson (1982) experimentally demonstrated a close, pressure-independent, relationship between apatite saturation and SiO_2 concentration in the melt, establishing P_2O_5 abundance as a function of silica content at which apatite starts crystallizing. This can be applied as a tool to estimate the minimum liquidus temperature using the whole rock P_2O_5 and SiO_2 contents. These experiments were performed in hydrous high-K calc-alkalic rocks, which make them applicable to estimate the minimum liquidus temperatures for these granitoids.

In the P_2O_5 vs. SiO_2 diagram (Fig. 11; superimposed isotherms after Green and Watson, 1982), data for these granitoids display a well-defined trend between 800 and 950 °C isotherms at 7.5 kbar pressure. This trend represents the temperature under which apatite started crystallizing, and approximates a near-liquidus temperature of the magma. Calculated values are in accord with estimates based upon the zircon saturation method.

In general, pressures and temperatures estimated by different methods are in mutual accord, and point toward moderately higher P–T conditions for granodiorites in relation to granites.

7. Oxygen fugacity estimate

The oxygen fugacity of the magma is closely governed by its source material, and it is difficult to use the end product (granitoids) to establish the oxygen fugacity of primary magmas. According to Enami et al. (1993), some inferences can be made using the rock mineral assemblage and mineral chemistry. Presence of Mg-rich amphiboles and early crystallizing biotite, euhedral titanite, and magnetite in felsic rocks indicate that the host magma was relatively oxidized. Wones (1989) also demonstrated that the titanite + magnetite + quartz assemblage in granitic rocks allows an estimate of relative oxygen fugacity, as follows:

$$\log fO_2 = -\mathbf{30930}/T + \mathbf{14.98} + \mathbf{0.142}(P-\mathbf{1})/T,$$

where T is temperature (Kelvin) and P is pressure (bar).

Accordingly, the above equation yields the lowest log oxygen fugacity for the Boqueirão pluton (−19 to −16), maximum for the Murici pluton (−17 to −14) and intermediate for the Conceição das Creoulas pluton (−17 to −18) (Table 5).

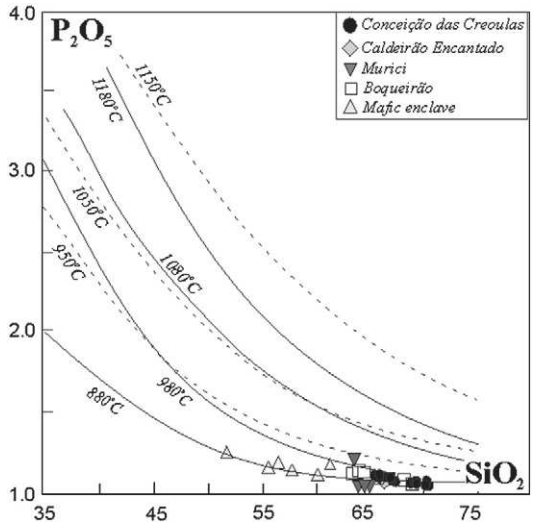

Fig. 11. Whole-rock P_2O_5 vs. SiO_2 plot for representative samples of the studied rocks displaying a trend between the 880 °C and 950 °C isotherms (dashed lines) at 7.5 kbar pressure (Green and Watson, 1982). Solid lines are for temperature as proposed by Watson (1980) for one atmosphere pressure.

8. Melt viscosity

Melt viscosity depends strongly upon chemical composition (especially SiO_2 content), temperature, and H_2O (and other volatile contents). An increase in temperature and water content decreases polymerization and lowers the viscosity of the melt. Under isothermal conditions, a lower SiO_2 content also decreases the viscosity. Decisive progress in the determination of the viscosity of hydrous silicate melts has been made in recent years, and several empirical equations are now available (e.g., Baker, 1998; Hess and Dingwell, 1996; Holtz et al., 2001). We have adopted the equation proposed by Baker (1998). Despite multiple factors affecting melt viscosity, the first-order parameters and the focus of available equations are H_2O, silica content, and temperature:

$$\log\eta_m = -\mathbf{1.86}\,XH_2O - \mathbf{0.09511}\,T + \mathbf{15.6293}$$

where T is the temperature in Kelvin, η_m is the viscosity in Pa.s, and XH_2O is mol%.

Baker (1998) has also suggested the following necessary conditions: (a) H_2O content between 0.3 and 12 wt.%, (b) SiO_2 in the range of 69–77 wt.%, (c) temperature between 577 and 1200 °C at crustal pressures. For XH_2O determination, he has proposed to use the Burnhan (1979) method.

We have considered samples with extreme and medium values of SiO_2 content (63.9 to 70.4%), and have used an inferred 3% water content based on the modal composition of hydrous minerals and the near-liquidus temperature of magma (based on the Zr saturation method; Watson, 1987). For the variation of water solubility (XH_2O) we have used the Burnhan (1979) equation as suggested by Baker (1998).

Calculated magmatic viscosities for these plutons vary from 1.1×10^4 to 4.6×10^4 Pa.s (Table 5).

9. Summary and conclusions

In these plutons, extraordinary structures—incipient semi-circular schlieren, ladder dikes, dioritic enclaves, and megacrystic aggregates aligned parallel to the regional foliation—are attributed to convective currents set up as underplating of mafic magma created temperature contrasts within the magma chamber (see Weinberg et al., 2001). The finer-scale oscillatory zoning and rows of biotite inclusions common in K-feldspar megacrysts also suggest origin in a convective magma chamber, or varying physico-chemical conditions during crystallization.

The four plutons are petrographically and mineralogically similar. Presence of early crystallizing hornblende, biotite, euhedral titanite, and magnetite indicates that the magma was relatively oxidized. Fe–Ti oxide minerals are rare—a common feature in the mEp granitoids in northeastern Brazil (see Sial et al., 1999). Schmidt and Thompson (1996) observed that magnetite is the main Fe^{3+} containing phase at temperatures above epidote stability, whereas at lower temperatures Fe^{3+} tends to enter epidote. In these plutons, it is probably true that epidote and titanite accommodated Fe^{3+} and Ti^{4+}: the magma did not

exhibit oxide saturation (Murici pluton is the only one which carries rare minute magnetite crystals).

The absence of alteration in biotite, and the fresh appearance of plagioclase in these plutons suggest that, in most of the cases, the rocks have been subjected to minimal weathering and low temperature (subsolidus) alteration, supporting an igneous origin for almost all epidote grains in these plutons.

The compositional variation of epidote (20–29% Ps) is consistent with values proposed by Johnston and Wyllie (1988), and by Tulloch (1979) for magmatic epidote. The Ps range of epidote in the Conceição das Creoulas pluton is consistent with crystallization around the NNO buffer, and the Ps range for epidote in the Conceição das Creoulas, Caldeirão Encantado, Boqueirão, and Murici plutons is consistent with crystallization between NNO and HM buffers. Minor to absent negative Eu anomalies also suggest that fO_2 was relatively high during magma crystallization. The highest values of oxygen activity (reflecting high water content of the magma) are recorded in the Murici pluton, and the lowest values are from the Boqueirão pluton.

The aluminum-in-hornblende barometer and hornblende–plagioclase thermometer indicate pluton emplacement within a pressure interval from 6 to 8 kbar (20–25 km). For these plutons, we estimate a solidus temperature between 620 and 780 °C based on plagioclase–hornblende pairs, and a near-liquidus temperature from 794 to 853 °C based on zircon saturation.

Presence of magmatic epidote in various textural relationships indicates extended temperature range of crystallization, above its stability field of ~6 kbar (Schmidt and Thompson, 1996), with subsequent rapid transport upward. Alternatively, the stability field of magmatic epidote could have extended to shallower crustal levels if fO_2 had been sufficiently high.

The observed positive correlations between Ba/Rb vs. Zr/Rb, and Zr/Rb vs. Sr/Rb are consistent with fractional crystallization as an important petrogenetic process according to Askren et al. (1997). Fusion of a hornblende-rich source, probably in the lower crust could have generated these high-K calc-alkalic and metaluminous to slightly peraluminous plutons. The similarities of mineralogy, bulk chemistry, and isotopic behavior ($\varepsilon Nd_{(0.60Ga)}$ from −2 to −5, T_{DM} from 1.2 to 1.3 Ga, very high $\delta^{18}O$ for zircon, quartz, and whole rock) for these plutons and mEp-bearing plutons elsewhere in the Cachoeirinha–Salgueiro and Alto Pajeú terranes (Ferreira et al., 2011; Sial, 1993; Sial et al., 1999) suggest similar origins in which a metabasaltic/mafic source interacted with water at low temperature.

In northeastern Brazil, magmatic epidote occurs both in some younger (0.58 Ga) and in older (0.65–0.63 Ga) plutons in the Transversal Zone (Ferreira et al., 2011), being more abundant and better preserved in the older group of plutons. Bittar (1999) estimated peak of metamorphic conditions for the western portion of the Alto Pajeú Terrane, at $P = 4.4 \pm 1.0$ kbar and $T = 700$ °C, conditions warmer than a normal continental geotherm (Brown, 2008). Leite et al. (2000) reported a concordant titanite U–Pb age of metamorphism of 612 ± 9 Ma for orthogneisses intrusive in the São Caetano complex in the Alto Pajeu Terrane. In the present study, survival of magmatic epidote happened at peak of metamorphism during the main stage of an orogenic cycle. Field relationships support similar ages for the four studied plutons, therefore, the assumption that rapid magma emplacement happened during peak of metamorphism likely applies to all four plutons.

Epidote survived less well in younger (0.58 Ga) plutons elsewhere that intruded a cooler environment after peak of metamorphism (Ferreira et al., 2011). The reason magmatic epidote has less chance of survival in magmas intruding cooler terranes (more brittle, more easily fracturing allowing magma dikes to shoot up fractures), while it survives better when magmas intruded warmer terranes, is an unanswered intriguing question.

Supplementary data associated with this article can be found, in the online version, at doi:10.1016/j.lithos.2011.09.017.

Acknowledgments

Grants from PADCT/FINEP (472132/2003-2), FINEP/FADE (1498/06) and FACEPE (APQ 0727-1.07/08) partially supported the field and laboratory work in this study. RGB acknowledges a three-year scholarship from the Brazilian Council for Scientific and Technological Development (CNPq). VPF thanks Gilsa M. Santana and Vilma S. Bezerra for helping with the oxygen isotope analyses at the LABISE. We are grateful to Mike Roden (University of Georgia, USA), Roberto F. Weinberg (Monash University, Australia) and especially thankful to Leon E. Long (University of Texas at Austin, USA) and an anonymous reviewer for important comments and suggestions made on an earlier version of the manuscript. All statements and conclusions here, however, are of the entire responsibility of the authors. This is the scientific contribution n. 241 of the NEG-LABISE, Department of Geology, Federal University of Pernambuco, Brazil.

References

Abbott Jr., R.N., 1985. Muscovite-bearing granites in the AFM liquidus projection. The Canadian Mineralogist 23, 553–561.
Abbott Jr., R.N., Clarke, D.B., 1979. Hypothetical liquidus relationships in the subsystem Al_2O_3–FeO–MgO projected from quartz, alkali feldspar and plagioclase for a $(H_2O) \leq 1$. The Canadian Mineralogist 17, 549–560.
Abdel-Rahman, A.F.M., 1994. Nature of biotites from alkaline, calc-alkalic, and peraluminous magmas. Journal of Petrology 35, 525–541.
Afifi, A.M., Essene, E.J., 1988. MINFILE: a microcomputer program for storage and manipulation of chemical data on minerals. American Mineralogist 73, 446–448.
Ague, J.J., 1987. Thermodynamic calculation of emplacement pressures for batholithic rocks, California: implications for the aluminum-in-hornblende barometer. Geology 25, 563–566.
Almeida, F.F.M., de Hasui, Y., Brito Neves, B.B., Fuck, R., 1981. Brazilian structural provinces: an introduction. Earth-Science Reviews 17, 1–29.
Anderson, J.L., 1996. Status of thermobarometry in granitic batholiths. Transactions of the Royal Society of Edinburg. Earth Science 87, 125–138.
Anderson, J.L., Smith, D.R., 1995. The effects of temperature and fO_2 on the Al-in-hornblende barometer. American Mineralogist 80, 549–559.
Argiolas, R., Baumer, A., 1978. Shynthèse de chloroapatite par voie hydrothermale: étude de l'influence de la saturation sur l"volution des faciès des cristaux. The Canadian Mineralogist 16, 285–290.
Askren, D.R., Roden, M.F., Whitney, J.A., 1997. Petrogenesis of tertiary andesite lava flows interlayered with large-volume felsic ash-flow tuffs of the western USA. Journal of Petrology 38, 1021–1046.
Baker, D.R., 1998. Granitic melt viscosity and dike formation. Journal of Structural Geology 20, 1395–1404.
Beurlen, H., da Silva Filho, A.F., Guimarães, I.P., Brito, S., 1992. Proterozoic C-type eclogites hosting unusual Ti–Fe–Cr–Cu mineralization in northeastern Brazil. Precambrian Research 58, 195–214.
Bittar, S.M.B., 1999. Faixa Pianco-Alto Brígida: terrenos tectonoestratigráficos sob regimes metamórficos deformacionais contrastantes. Unpublished doctoral thesis, University of São Paulo, Institute of Geosciences, 126p.
Blundy, J.D., Holland, T.J.B., 1990. Calcic amphibole equilibria and a new amphibole–plagioclase geothermometer. Contributions to Mineralogy and Petrology 104, 208–224.
Brandon, A.D., Creaser, R.A., Chacko, T., 1996. Constraints on rates of granitic magma transport from epidote dissolution kinetics. Science 271, 1845–1848.
Brasilino, R.G., Sial, A.N., Lafon, J.M., 1999. Magmatic epidote, hornblende barometric estimates, and emplacement of the Conceição das Creoulas pluton, Alto Pajeú terrane, NE Brazil. Anais da Academia Brasileira de Ciências 71, 4–16.
Brito Neves, B.B., Santos, E.J., Van Schmus, W.R., 2000. Tectonic history of the Borborema province, northeastern Brazil. In: Cordani, U.G., Milani, E.J., Thomaz Filho, A., Campos, D.A. (Eds.), 31st International Geological Congress, Rio de Janeiro, pp. 151–182.
Brito Neves, B.B., Van Schmus, W.R., Santos, E.J., Campos Neto, M.C., Kozuch, M., 1995. O Evento Cariris Velhos na Província da Borborema: integração de dados, implicações e perspectivas. Revista Brasileira de Geociencias 25, 279–296.
Brito Neves, B.B., Guimarães, I.P., Santos, E.J., Van Schmus, W.R., Campos Neto, M.C., 2003. Geology, geochemistry and geochronology (Rb–Sr, U–Pb, Sm–Nd and Ar–Ar) of the orthogneisses from the Alto Pajeú Terrane. IV South American Symposium on Isotopic Geology. Salvador. Short Papers—IV SSAGI, 1. Companhia Baiana de Pesquisa Mineral, Salvador, pp. 155–157.
Brown, M., 2008. Characteristic thermal regimes of plate tectonics and their metamorphic in print throughout Earth history: when did Earth first adopted a plate tectonic mode of behavior? Geological Society of America Special paper 440, 97–128.
Burnhan, C.W., 1979. The importance of volatile constituents. In: Yoder, H.S. (Ed.), The Evolution of the Igneous Rocks: Fiftieth Anniversary Perspectives. Princeton University Press, Princeton, N.J, pp. 439–482.
da Silva Filho, A.F., Guimarães, I.P., Thompson, R.N., 1993. Shoshonitc and ultrapossic Proterozoic intrusive suites in the Cachoeirinha–Salgueiro Belt, NE, Brazil: a transition from collisional to postcollisional magmatism. Precambrian Research 62, 323–342.

dos Santos, E.J., Medeiros, V.C., 1999. Constraints from granitic plutonism on Proterozoic crustal growth of the transverse zone, Borborema Province NE Brazil. Revista Brasileira de Geociencias 29, 73–84.
dos Santos, E.J., Brito Neves, B.B., Van Schmus, W.R., 1995. O complexo granítico Lagoadas Pedras: acresção e colisão na região de Floresta (Pernambuco), Província Borborema. Simpósio de Geologia do Nordeste, 16, 1995, Recife. : Atas, XVI Simpósio de Geologia do Nordeste, 14. Sociedade Brasileira de Geologia, Recife, pp. 401–406.
dos Santos, E.J., Oliveira, R.G., Paiva, I.P., 1997. Terrenos no domínio transversal da Província da Borborema: controles sobre acresção e retrabalhamento crustais ao sul do lineamento Patos. XVII Simposio de Geologia do Nordeste, Fortaleza, Resumo Expandido, 2. Sociedade Brasileira de Geologia, Fortaleza, pp. 401–406.
dos Santos, E.J., Van Schmus, W.R., Kozuch, M., Brito Neves, B.B., 2010. The Cariris Velhos tectonic event in Northeast Brazil. Journal of South American Earth Sciences 29, 61–76.
Enami, M., Suzuki, K., Liou, J.G., Bird, D.K., 1993. Al–Fe^{3+} and F–OH substitutions in titanite and constraints on their P–T dependence. European Journal of Mineralogy 5, 219–231.
Evans, B.W., Patrick, B.E., 1987. Phengite-3T in high-pressure metamorphosed granitic orthogneisses, Seward Peninsula, Alaska. The Canadian Mineralogist 25, 141–158.
Ferreira, V.P., Sial, A.N., 1997. Two distinct sources for ultrapotassic magmas in the Transverse Zone, northeastern Brazil: oxygen and Nd isotopes. Semana de Geoquímica, 10, Congresso de Geoquimica dos Países de Lingua Portuguesa, 4, Braga,1997, Actas., Braga, 43.
Ferreira, V.P., Sial, A.N., Whitney, J.A., 1994. Large-scale silicate liquid immiscibility: a possible example from northeastern Brazil. Lithos 33, 285–302.
Ferreira, V.P., Sial, A.N., Jardim de Sá, E.F., 1998. Geochemical and isotopic signatures of Proterozoic granitoids in terranes of Borborema structural province, northeast Brazil. Journal of South American Earth Sciences 11, 439–455.
Ferreira, V.P., Valley, J.W., Sial, A.N., Spicuzza, M., 2003. Oxygen isotope compositions and magmatic epidote from two contrasting metaluminous granitoids, NE Brazil. Contributions to Mineralogy and Petrology 145, 205–216.
Ferreira, V.P., Sial, A.N., Pimentel, M.M., Moura, C.A.V., 2004. Intermediate to acid magmatism and crustal evolution in the Transversal Zone, Northeastern Brazil. Geologia de Continente Sul-Americano: Evolução da obra de Fernando Flávio de Almeida, pp. 190–201.
Ferreira, V.P., Sial, A.N., Pimentel, M.M., Armstrong, R., Spicuzza, M., Guimarães, I., Silva Filho, A.F., 2011. Contrasting sources and P–T crystallization conditions of epidote-bearing granitic rocks, Northeastern Brazil: O, Sr and Nd isotopes. Lithos 121, 189–201.
Fetter, A.H., Van Schums, W.R., dos Santos, T.J.S., Arhaud, M., Nogueira Neto, J.A., 2000. U–Pb and Sm–Nd geochronological constraints on the crustal evolution and basement architecture of Ceará state, NW Borborema Province, NE Brazil: implications of the existence of Palaeoproterozoic supercontinent Atlantica. Revista Brasileira de Geociencias 30, 102–106.
Franz, G., Spear, E.S., 1985. Aluminous titanite (sphene) from the eclogite-zone, south central Tauern Window, Austria. Chemical Geology 50, 33–46.
Girault, J., 1966. Génese et géochimie de l'apatite et de la calcite dans les roches liées au complexe carbonatitique et hyperalcalin d'Oka (Canada). In Conceição, H. 1990. Petrologie du massif syénitic d'Itiuba: contribuition a l'étude minéralogique des roches alcalines dans l'état de Bahia (Brazil). Université Paris-Sud, Centre d'Orsay, These doct., 395p.
Green, T.H., Watson, E.B., 1982. Crystallization of apatite in natural magmas orogenic rock series. Contributions to Mineralogy and Petrology 79, 96–105.
Hackspacker, P.C., Van Schums, W.R., Dantas, E.I., 1990. Um embasamento Transamazonico na Provincia Borborema. Congresso Brasileiro de Geologia 36, Natal, Anais, pp. 2683–2696.
Hammarstrom, J.M., Zen, E-An, 1983. Possible use of Al content in hornblende as geobarometer for plutonic rocks. Geological Society of America, Annual Meeting, Abstracts with Programs, Indianapolis, 590.
Hammarstrom, J.M., Zen, E-An, 1986. Aluminum in hornblende: an empirical igneous geobarometer. American Mineralogist 71, 1297–1313.
Hess, K.U., Dingwell, D.B., 1996. Viscosities of hydrous leucogranitic melts. A non Arrhenian model. American Mineralogist 81, 1297–1300.
Holland, T.J.B., Blundy, J.D., 1994. Non-ideal interaction in calcic-amphiboles and their bearing on amphibole-plagioclase thermometry. Contributions to Mineralogy and Petrology 116, 433–447.
Hollister, L.S., Grisson, G., Peters, E.K., Stowell, H.E., Sisson, V.B., 1987. Confirmation of the empirical correlation of Al in hornblende pressure of solidification of calc-alkalic plutons. American Mineralogist 72, 231–239.
Holtz, F., Johannes, W., Tamic, N., Behrens, H., 2001. Maximum and minimum water contents of granitic melts generated in the crust: a reevaluation and implications. Lithos 56, 1–14.
Ishihara, S., 1977. The magnetite-series and ilmenite-series granitic rocks. Mining Geology 27, 293–305.
Johnston, A.D., Wyllie, P.J., 1988. Constraints on the origin of Archean trondhjemites based on phase relationships of Nuk gneiss with H2O at 15 kbar. Contributions to Mineralogy and Petrology 100, 35–46.
Johnson, M.C., Rutherford, M.J., 1989. Experimental calibration of the aluminum-in-hornblende geobarometer with application to Long Valley caldera (California) volcanic rocks. Geology 17, 837–841.
Lackey, J.S., Valley, J.W., Chen, J.H., Stockli, D.F., 2008. Dynamic magma systems, crustal recycling, and alteration in the Central Sierra Nevada Batholith: the oxygen isotope record. Journal of Petrology 49, 1397–1426.
Lameyre, J., Bowden, P., 1982. Plutonic rocks types series: discrimination of various granitoid series and related rocks. In: Brousse, R., Lameyre, J. (Eds.), Magmatology: Journal of Volcanology and Geothermal Research, 14, pp. 169–186.
Leake, B.E., 1978. Nomenclature of amphiboles. American Mineralogist 63, 1023–1052.
Leake, B.E., 1997. Nomenclature of amphiboles: report of the subcommittee on amphiboles of the International Mineralogical Association, Commission on New Minerals and Mineral Names. American Mineralogist 82, 1019–1037.
Leite, P.R.B., Bertrand, J.M., Lima, E.S., Leterrier, J., 2000. Timing of granitic magmatism in the northern Borborema province, Brazil: a U–Pb study of granitoids from the Alto Pajeú terrain. Journal of South American Earth Sciences 13, 549–559.
Liou, J.G., 1973. Synthesis and stability relations of epidote, $Ca_2Al_2FeSiO_3O_{12}(OH)$. Journal of Petrology 14, 381–413.
Mariano, G., Neves, S.P., Silva Filho, A.F., da Guimarães, I.P., 2001. Diorites of the high-calc-alkalic association: geochemistry and Sm-Nd data and implications for the evolution of the Borborema Province, Northeast Brazil. International Geology Review 43, 921–929.
Mariano, G., Correia, P.B., Neves, S.P., Silva Filho, A.F., 2009. The high-K calc-alkaline Alagoinhas pluton: anisotropy of magnetic susceptibility, geochemistry, emplacement setting, and implications for the evolution of Borborema Province, NE Brazil. International Geology Review 51, 502–519.
Mason, G.H., 1985. The mineralogy and textures of the Coastal Batholith, Peru. In: Pitcher, W.S., Atherton, M.P., Cobbing, E.J., Beckinsale, R.D. (Eds.), Magmatism at a Plate Edge: The Peruvian Andes. Blackie Halstead Press, Glasgow, pp. 156–166.
Muehlenbachs, K., Valley, J.W., Taylor Jr., H.P., O'Neil, J.R., 1986. Alteration of the oceanic crust and the 18O history of seawater. Stable isotopes in high temperature geological processes. Reviews in Mineralogy, Mineralogical Society of America, Washington, DC., USA, pp. 425–444.
Nachit, H., Razafimahefa, N., Stussi, J.M., Carron, J.P., 1985. Composition chimique des biotites et typologie magmatique des granitoides. Comptes Rendus de l´Académie des Sciences de Paris série II 301 (11), 813–818.
Naney, M.T., 1983. Phase equilibria of rock-forming ferromagnesian silicates in granitic systems. American Journal of Science 283, 993–1033.
Neves, S.P., 2000. Província Borborema: uma colagem de terrenos ou orógeno intracontinental? XVIII Simpósio de Geologia do Nordeste, Recife, Resumos, 139.
Neves, S.P., Mariano, G., Guimarães, I.P., Silva filho, A.F., da Melo, S.C., 2000. Intralithospheric differentiation and crustal growth: evidence from the Borborema province, northeastern Brazil. Geology 28, 519–522.
Neves, S.P., Bruguier, Olivier, da Silva, José, Rangel, Maurício, Bosch, Delphine, Alcantara, V.C., Lima, Cristiane Marques, 2009. The age distributions of detrital zircons in metasedimentary sequences in eastern Borborema Province (NE Brazil): evidence for intracontinental sedimentation and orogenesis? Precambrian Research 175, 187–205.
O'Neil, J., Shaw, S.F., Flood, R.H., 1977. Oxygen and hydrogen isotope compositions of granite genesis in the New England batholith, Australia. Contributions to Mineralogy and Petrology 62, 313–325.
Richard, L., 1995. The Ultimate Mineralogical and Petrological, Data Processing System for Windows, Minpet Geological Software—Logiciel Geologique. Minpet, Quebec.
Roberts, M.P., Clemens, J.D., 1993. The origin of high potassium, calc-alkaline, I-type granitoids. Geology 21, 825–828.
Rodrigues, S.W.O., Brito Neves, B.B., 2008. Padrões Isotópicos Sm–Nd no limite entre os terrenos Alto Pajeú e Alto Moxotó (PB). Revista Brasileira de Geociências 38, 209–225.
dos Santos, E.J.2000. Programa de Levantamentos Geológicos Básicos do Brasil. Belém do São Francisco. Folha SC.24-X-A. Estado de Pernambuco, Alagoas e Bahia. Escala 1: 250.000. Geologia e Metalogênese. Recife, Companhia de Pesquisa de Recursos Minerais (CD ROM).
dos Santos, E.J., Nutman, A.P., Brito Neves, B.B., 2003. U–Pb SHRIMP ages of the Sertânia Complex: implications on tectonic framework of the Transversal subprovince, Northeast Brazil. IV South American Symposium on Isotope Geology, 2003, Salvador BA, 1. Companhia Bahiana de Pesquisa Mineral, Salvador BA, pp. 274–277 (Short Papers).
Schmidt, M.W., 1992. Amphibole composition in tonalite as a function of pressure: an experimental calibration of the Al-in-hornblende-barometer. Contributions to Mineralogy and Petrology 110, 304–310.
Schmidt, M.W., Thompson, A.B., 1996. Epidote in calc-alkalic magmas: an experimental study of stability phase relationships, and the role of epidote in magmatic evolution. American Mineralogist 81, 462–474.
Sial, A.N., 1986. Granite-types in Northeast Brazil: current knowledge. Revista Brasileira de Geociencias 16, 54–72.
Sial, A.N., 1993. Contrasting metaluminous magmatic epidote-bearing granitic suites from two Precambrian Foldbelts in Northeast Brazil. Anais Academia Brasileira Ciencias 65 (suppl.1), 141–162.
Sial, A.N., Toselli, A.J., Saavedra, J., Ferreira, V.P., 1999. Emplacement, petrological and magnetic susceptibilty characteristics of diverse magmatic epidote-bearing granitoid rock in Brazil, Argentina and Chile. Lithos 46, 367–392.
Sial, A.N., Vasconcelos, P.M., Ferreira, V.P., Pessoa, R.R., Brasilino, R.G., Morais Neto, J.M., 2008. Geochronological and mineralogical constraints on depth of emplacement and ascension rates of epidote-bearing magmas from northeastern Brazil. Lithos 105, 225–238.
Speer, J.A., 1987. Evolution of magmatic AFM mineral assemblages in granitoid rocks: the hornblende + melt = biotite reaction in the Liberty Hill Pluton, South Carolina. American Mineralogist 72, 863–878.
Streckeisen, A., 1976. To each plutonic rock its proper name. Earth-Science Reviews 12, 1–33.
Takahashi, M., Aramaki, S., Ishihara, S., 1980. Magnetite-series/ilmenite series vs. I-type/S-type granitoids. Mining Geology Special Issue 8, 13–28.
Tropper, P., Manning, C.E., Essene, E.J., 2002. The substitution of and F in titanite at high pressure and temperature: experimental constraints on phase relations and solid solution properties. Journal of Petrology 43, 1787–1814.
Tulloch, A., 1979. Secondary Ca–Al silicates as low-grade alteration products of granitoid biotite. Contributions to Mineralogy and Petrology 69, 105–117.

Valley, J.W., Chiarenzelli, J.R., McLelland, J.M., 1994. Oxygen isotope geochemistry of zircon. Earth and Planetary Science Letters 126, 187–206.
Van Schmus, W.R., Brito Neves, B.B., Hackspacker, P.C., Babinski, M., 1995. U/Pb and Sm/Nd geochronologic studies of the eastern Borborema province, northeastern Brazil: initial conclusions. Journal of South American Earth Sciences 8, 267–288.
Vyhnal, C.R., McSween Jr., H.Y., Speer, J.A., 1991. Hornblende chemistry in southern Appalachian granitoids: implications for aluminum hornblende thermobarometry and magmatic epidote stability. American Mineralogist 76, 176–188.
Watson, E.B., 1980. Apatite saturation in basic to intermediate magmas. Geophysical Research Letters 6, 937–940.
Watson, E.B., 1987. The hole of accessory minerals in granitoid geochemistry. Hutton Conference of the Origin of Granites: Transactions of the Royal Society of Edinburgh, pp. 209–211.
Watson, E.B., Harrison, M.T., 1984. Zircon saturation revisited: temperatures and composition effects in a variety of crustal magma types. Earth and Planetary Science Letters 104, 381–397.
Weinberg, R.F., Sial, A.N., Pessoa, R.R., 2001. Magma flow within the Tavares pluton northeastern Brazil: compositional and thermal composition. Geological Society of America Bulletin 113, 508–520.
Weinberg, R.F., Sial, A.N., Mariano, G., 2004. Close spatial relations between plutons and shear zones. Geology 32, 337–380.
Wones, D.R., 1989. Significance of the assemblage titanite + magnetite + quartz in granitic rocks. American Mineralogist 74, 744–749.
Wyllie, P.J., Cox, K.G., Biggar, G.M., 1962. The habit of apatite in synthetic systems and igneous rocks. Journal of Petrology 3, 238–243.
Yavuz, F., 1998. New Amphical: A Program to Classify Microprobe Wet Chemical Amphibole Analyses. (PK. 90, 81302. Kadikõy, Istanbul,Turkey) .
Yavuz, F., 2001. LIMICA: a program for estimating Li from electron-microprobe mica analyses and classifying trioctahedral micas in terms of composition and octahedral site. Computer and Geosciences 12, 215–227.
Zen, E-an, 1988. Tectonic significance of high pressure plutonic rocks in the Western Cordillera of North America. In: Ernst, W.G. (Ed.), Metamorphism and Crustal Evolution of the Western United States, Rube, vol. VIII. Prentice-Hall, Engelwood Cliffs, New Jersey, pp. 41–71.
Zen, E-An, Hammarstrom, J.M., 1984. Magmatic epidote and its petrologic significance. Geology 12, 515–518.